

Published in final edited form as:

Neuron. 2009 November 12; 64(3): . doi:10.1016/j.neuron.2009.08.036.

A Functional Mouse Retroposed Gene *Fg01* Reduces Alzheimer's β -Amyloid Levels and Tau Phosphorylation

Yun-wu Zhang^{1,2,8}, Shijie Liu^{2,8}, Xue Zhang^{2,8}, Wu-Bo Li^{3,8}, Yaomin Chen², Xiumei Huang^{1,2}, Liangwu Sun², Wenjie Luo⁴, William J. Netzer⁴, Richard Threadgill³, Gordon Wiegand³, Ruishan Wang^{1,2}, Stanley N. Cohen⁵, Paul Greengard⁴, Francesca-Fang Liao^{2,7}, Limin Li^{3,6,*}, and Huaxi Xu^{2,*}

¹Institute for Biomedical Research and Fujian Provincial Key Laboratory of Neurodegenerative Disease and Aging Research, Xiamen University, Xiamen 361005, China

²Neurodegenerative Disease Research Program, Burnham Institute for Medical Research, La Jolla, CA 92037, USA

³Functional Genetics, Inc., Gaithersburg, MD 20878, USA

⁴Laboratory of Molecular and Cellular Neuroscience, The Rockefeller University, New York, NY 10065, USA

⁵Department of Genetics, Stanford University School of Medicine, Stanford, CA 94305, USA

⁶Department of Pathology, Institute of Basic Medical Sciences, Chinese Academy of Medical Sciences & Peking Union Medical College, Beijing 100005, China

⁷Department of Pharmacology, University of Tennessee Health Science Center College of Medicine, Memphis, TN 38163, USA

SUMMARY

Senile plaques consisting of β -amyloid (A β) and neurofibrillary tangles composed of hyperphosphorylated tau are major pathological hallmarks of Alzheimer's disease (AD). Elucidation of factors that modulate A β generation and tau hyperphosphorylation is crucial for AD intervention. Here we identify a novel mouse gene *Fg01* that originated through retroposition of ribosomal protein S23. We demonstrate that FG01 protein reduces the levels of A β and tau phosphorylation by interacting with adenylate cyclases to activate cAMP/PKA and thus inhibit GSK-3 activity. The function of *Fg01* is demonstrated in cells of various species including human, and in transgenic mice overexpressing FG01. Furthermore, the AD-like pathologies of triple transgenic AD mice were improved and levels of synaptic marker proteins increased after crossing them with *Fg01* transgenic mice. Our studies reveal a new target/pathway for regulating AD pathologies and uncover a novel retrogene and its role in regulating protein kinase pathways.

© 2009 Elsevier Inc. All rights reserved.

*Correspondence: xuh@burnham.org (H.X.) or limin@liminli.com (L.L.).

⁸These authors contributed equally to this work

Publisher's Disclaimer: This is a PDF file of an unedited manuscript that has been accepted for publication. As a service to our customers we are providing this early version of the manuscript. The manuscript will undergo copyediting, typesetting, and review of the resulting proof before it is published in its final citable form. Please note that during the production process errors may be discovered which could affect the content, and all legal disclaimers that apply to the journal pertain.

INTRODUCTION

Alzheimer's disease (AD) is featured by extracellular neuritic plaques, intracellular neurofibrillary tangles (NFTs), synaptic dysfunctions and neural degeneration in vulnerable brain regions (Tanzi and Bertram, 2005). Neuritic plaques are composed of aggregates of heterogeneous β -amyloid ($A\beta$) peptides, which are derived from β -amyloid precursor protein (APP) through sequential cleavages by β -secretase (BACE1) and the γ -secretase complex (consisting of at least four components: presenilin, nicastrin, APH-1 and PEN-2) (Cole and Vassar, 2007; De Strooper, 2003; Zhang and Xu, 2007). Multiple lines of evidence suggest that overproduction/aggregation of $A\beta$ in the brain is a causative factor for AD pathogenesis (Hardy and Selkoe, 2002). NFTs are composed of hyperphosphorylated microtubule associated protein tau (Buee et al., 2000; Lee et al., 2001). Numerous studies have shown that pathogenic APP metabolism/ $A\beta$ generation and tau phosphorylation are highly regulated via various signal transduction pathways, e.g., protein kinases and phosphatases (Buxbaum et al., 1994; Fang et al., 2000; Xu et al., 1996) and steroid and peptide hormones (Gasparini et al., 2001; Xu et al., 1998). Among these regulatory pathways, glycogen synthase kinase-3 (GSK-3, α and β isoforms), a serine/threonine kinase essential for a variety of cellular functions including cell adhesion, cell-division, transcription (Frame and Cohen, 2001), has been demonstrated in regulating both $A\beta$ generation and tau phosphorylation (Flaherty et al., 2000; Phiel et al., 2003). This unique feature renders manipulation of GSK-3 activity an attractive therapeutic approach for AD (Frame and Cohen, 2001; Martinez et al., 2002; Medina and Castro, 2008). Hence identification of new genes involved in these processes will be instrumental in developing novel AD therapeutics.

The creation of genetic novelty by the formation of new genes has an important role in evolution. New genes can originate through different mechanisms that include exon shuffling, gene duplication, gene fusion/fission, mobile element integration, lateral gene transfer, and retroposition (Long et al., 2003). Retroposition is a process in which a parental mRNA is reverse-transcribed and inserted into the organism's genome, creating duplicate genes in new genomic positions (Hollis et al., 1982; Karin and Richards, 1982; Ueda et al., 1982). Although these intronless retroposed gene copies commonly lack the regulatory elements of parental genes and thus routinely have been classified as processed pseudogenes (Jeffs and Ashburner, 1991; Mighell et al., 2000; Zhang et al., 2004), occasionally, these retroposed gene copies can recruit regulatory elements as well as protein-encoding sequences at or near the retroposition site and become expressed and functional (Babushok et al., 2007; Kaessmann et al., 2009; Long et al., 2003; Vinckenbosch et al., 2006). Nevertheless, studies to elucidate the functions of these newly originated genes, especially the functions related to diseases, are limited (Kaessmann et al., 2009; Vinckenbosch et al., 2006).

Random Homozygous Gene Perturbation (RHGP, previously called Random Homozygous Knockout, RHKO) is a genome-wide genetic approach that identifies genes based on their biological functions (Li and Cohen, 1996; Liu et al., 2000a; Liu et al., 1999; Liu et al., 2000b). The design of RHGP enables the inactivation of both alleles of randomly addressed chromosomal genes within populations of mammalian cells using gene search vector cassettes that contain a regulated antisense promoter. This strategy has been used successfully to identify genes whose functional homozygous inactivation leads to reversible tumorigenesis (Li and Cohen, 1996; Liu et al., 2000a; Liu et al., 1999; Liu et al., 2000b), or altered sensitivity to chemotherapeutic agents (Lih et al., 2006).

Here using the RHGP approach, we identified a novel gene *Fg01* that originated through retroposition of the mouse ribosomal protein S23 (*Rps23*) mRNA. The *Fg01* gene is reversely transcribed relative to its parental gene, expressing a structurally unrelated, yet

functional protein FG01. More importantly, we demonstrated both *in vitro* and *in vivo* that overexpression of the FG01 protein decreases the levels of A β and tau phosphorylation and increases synaptic marker proteins in AD transgenic mice, by inhibiting GSK-3 activity via the adenylate cyclase/protein kinase A (PKA) pathway.

RESULTS

Genome-wide Screening for Genes that Regulates A β Generation

It has been shown that reduction of A β levels is accompanied by cell surface accumulation of APP β CTF (the product of β -cleavage and immediate substrate for γ -cleavage), which is readily detectable in cells deficient in PS1 (Chen et al., 2000); and these cells can be identified using an antibody specifically recognizing the N-terminus of APP β CTF (FCA18) (Ancolio et al., 1999). Based on this observation, we adapted RHGP as a high throughput screen to search for genes that regulate A β generation.

We modified the original vector pLLGSV (Li and Cohen, 1996) to increase efficiency of retroviral integration and gene recovery. The new RHGP gene search vector contains modified LTRs and utilizes the Cre-*LoxP* mediated recombination to minimize promoter interference in provirus and to facilitate genomic DNA cloning (Figure 1A). This vector was transfected into Phoenix-Ampho cells for viral packaging. Harvested retrovirus was used to infect mouse neuroblastoma N2a cells stably expressing the human APP Swedish mutation (N2aSwe). After random insertion, the provirus (Figure 1B) expressed Cre recombinase for recognition and recombination of the two *LoxP* sites located in the 5'LTR and 3'LTR, respectively, generating the final integrated provirus (Figure 1C). A tetracycline regulated promoter (TRE-CMV) promoter in the final integrated provirus drives the expression of *Pac* for puromycin selection and initiates transcription into flanking chromosomal gene that can either overexpress, when TRE-CMV is in the same orientation, or suppress (by expressing antisense transcripts) when TRE-CMV is in the opposite orientation relative to the flanking gene. Moreover, transcription of the tetracycline-regulated (*tet-off*) transactivator was reversed in the presence of tetracycline (or doxycycline).

Therefore, we first acquired N2aSwe cells with stable integration of the RHGP search vector by puromycin selection. These cells were live-immunostained with fluorescently labeled FCA18 antibody followed by multiple rounds of FACS sorting to enrich for cells showing surface APP β CTF accumulation. Less than 0.01% of cells showing β CTF accumulation after first round of FACS sorting were enriched up to 75% following another two rounds of FACS sorting (Figure 2A). These cells were then sorted with additional FACS in the presence of doxycycline for a reversion of cell surface APP β CTF to background level to eliminate potential false positive. The final sorted cells were cloned individually, propagated and assayed for both accumulated cell surface APP β CTF and reduced A β generation. This screening strategy is shown in Figure 1D.

Identification of the *Fg01* Gene

One clone, FG01, was isolated for the high level of cell surface APP β CTF and the significant reduction of A β secretion (Figures 2B and 2C). Both phenotypes were reversed by doxycycline treatment, validating that the effects were indeed a result of RHGP rather than cell-cell/clonal variation in APP/ β CTF expression or any random mutagenesis (Figure 2C). Subcloning and sequence analyses revealed that the RHGP vector was inserted into chromosome 8 at a site ~1.2Kb upstream of the *C330021F23Rik* gene (GenBank ID: 546049), which has no known function. We herein designated this gene as *Fg01*. The upstream location and the same orientation of the inserted RHGP vector strongly suggested that *Fg01* was likely overexpressed in this cell clone. This notion was supported by real-time

reverse transcription-PCR (RT-PCR) using RNAs from parental N2aSwe and the FG01 RHGP cell clone, which showed that *Fg01* was overexpressed in the FG01 RHGP cell clone and its overexpression was reversed by doxycycline treatment (Figure 2D).

The *Fg01* gene is predicted to encode a 141 amino acid-long hypothetical protein that we designate FG01. Interestingly, analyses of multiple genome databases (GenBank, UCSC Genome Browser and Ensemble Genome Browser) with the FG01 protein sequence identified no FG01 homologs in other species including humans and rats. Further analysis with the *Fg01* gene sequence showed that the predominant protein-encoding region of the *Fg01* gene was highly homologous to the reverse and complementary sequence of the mouse ribosomal protein S23 (*Rps23*) mRNA (Figure 3A). The similarity between *Fg01* and mouse *Rps23* was even higher than those between mouse *Rps23* and rat or human *Rps23* (Figure 3B), suggesting that *Fg01* originated from mouse *Rps23* after the divergence of mice and rats. New genes can originate through different mechanisms (Long et al., 2003). However, the presence of the mouse *Rps23* untranslated regions (UTRs) and the absence of the mouse *Rps23* introns in the homologous regions between *Fg01* and mouse *Rps23* clearly suggest that *Fg01* originated through retroposition of the mouse *Rps23* mRNA, which recruited regulatory units and additional protein-encoding sequence near the retroposition site. But transcription of *Fg01* is reversed compared to *Rps23*. To search for human homologs of *Fg01*, we scanned the human genome with the human *Rps23* cDNA sequence and identified several *Rps23* retroposition sites (Figure S1). However, computational gene prediction of these sites revealed no functional *Fg01*-like genes. We also carried out RT-PCR with primers binding regions right next to these human *Rps23* retroposition sites and failed to obtain positive amplification (data not shown).

FG01 is a Type Ib Transmembrane Protein

Bioinformatics analysis using the FG01 amino acid sequence predicted a helical transmembrane domain near the C-terminus but no obvious signal peptide sequence. We constructed a vector expressing recombinant FG01 with a Myc tag at the N-terminus and a His₆ tag at the C-terminus (Myc-FG01-His₆, Figure 4A). Both Myc and His₆ antibodies recognized a product of approximately 17 kDa in transfected Myc-FG01-His₆ cells, consistent with the predicted molecular weight, indicating that there is no cleavable signal peptide sequence within FG01 (Figure 4B). Furthermore, after transfection of Myc-FG01-His₆ vector into N2a cells, fractionation of cell lysates into cytosolic and membrane components indicated that the majority of FG01 protein was located in membrane fractions (Figure 4C). Biotinylation assays also revealed that FG01 was delivered to the cell surface (Figure 4D). To determine FG01 topology, we transfected N2a cells with the Myc-FG01-His₆ vector and immunostained either live cells or cells after permeabilization, using antibodies against Myc or His₆. Our results show that although both antibodies were immunoreactive in permeabilized cells, only the Myc antibody positively stains the membranes of live cells, whereas the His₆ antibody does not, suggesting that the FG01 N-terminus is extracellular (Figure 4E). Hence these results suggest that FG01 is a type Ib transmembrane protein that has a normal type I transmembrane protein orientation but no signal peptides. Immunoprecipitation combined with live-immunostaining also confirmed the type Ib transmembrane topology of FG01 (Figure S2). We derived an antibody against the N-terminus of FG01 (Figure S3) and using this antibody for immunoprecipitation followed by Western blot analysis, we confirmed expression of FG01 in both cortex and hippocampus (Figure 4F). *In situ* hybridization analysis of *Fg01* expression in mouse brain revealed that *Fg01* is indeed expressed primarily in hippocampus, dentate gyrus, and cortex (Figure 4G).

FG01 Overexpression Reduces A β Levels, GSK-3 Activity and Tau Phosphorylation

The FG01 RHGP cell clone exhibits increased APP β CTF accumulation and reduced A β levels (Figure 2C), suggesting that FG01 regulates APP processing. To corroborate this, we overexpressed FG01 in N2aSwe cells. The results showed that, although the levels of total APP were not affected, the levels of extracellular and intracellular A β were significantly reduced by FG01 overexpression, and the levels of β CTF and sAPP α were significantly increased (Figure 5A). When human HeLa cells stably expressing the human APP Swedish mutation (HeLaSwe) were transfected with mouse FG01, we also observed reduced A β levels and increased accumulation of β CTF and sAPP α (Figure 5A). ELISA analysis confirmed that both A β 40 and A β 42 levels were significantly reduced following FG01 expression in HeLaSwe cells (Figure 5B). These data demonstrated that mouse FG01 can function not only in mouse cells, but also in human cells.

To determine whether FG01 reduces A β levels by modulating β -secretase activities, we examined β -secretase (BACE1) activity and the protein level of BACE1 *in vitro* in FG01-overexpressing cells and found them both unchanged (Figures S4A and S4B). APP β CTF accumulation can also be attributed to a decrease in γ -secretase-mediated cleavage. However, cleavage of Notch, another important γ -secretase substrate (Kopan and Goate, 2000), was not altered by FG01 overexpression (Figure S4C). Protein levels of nicastrin, an important component of the γ -secretase complex, and ADAM10 and TACE, two putative α -secretases (Zhang and Xu, 2007), were also not affected by FG01 overexpression (Figure S4B).

Although the possibility that FG01 may modulate substrate specificity or accessibility to γ -secretase can not be excluded, it is equally possible that FG01 regulates other proteins/pathways functioning in APP processing and A β generation. One of those could be GSK-3, which has been shown to affect A β generation (without affecting γ -secretase-mediated Notch cleavage) and tau phosphorylation (Phiel et al., 2003; Takashima et al., 1995). Thus, we studied the activities of GSK-3 α/β in the presence or absence of FG01 overexpression by examining levels of phospho-GSK-3 α (Ser 21) and phospho-GSK-3 β (Ser 9) (which represent inactivated forms of GSK-3) and by *in vitro* kinase assays. In cells overexpressing FG01 we observed that GSK-3 α/β was more highly phosphorylated at these sites in mouse N2aSwe (Figure 5A), rat PC12 (data not shown), and human HeLaSwe (Figure 5A) and HEK293 (data not shown) cells, indicating that FG01 can decrease GSK-3 kinase activity in cells of various types and species including human. *In vitro* kinase assays also demonstrated an approximately 50% decrease in GSK-3 α and a 40% decrease in GSK-3 β activities in FG01-overexpressing cells (Figure 5C). Remarkably, in the presence of lithium, a general inhibitor of both GSK-3 α and GSK-3 β , FG01 overexpression could not further reduce GSK-3 α/β activity or A β production (Figure 5D). These data suggest that FG01 reduces A β levels by downregulating GSK-3 activity.

GSK-3 is a major kinase that phosphorylates tau in AD (Flaherty et al., 2000). Hence, we asked whether FG01 affects tau phosphorylation by inhibiting GSK-3. We cotransfected N2aSwe cells with the human tau splice variant T40 and with FG01 (or control vectors), and examined tau phosphorylation at the threonine 205 site (pT205) and the PHF-1 tau epitope sites (serine 396 and serine 404), which are GSK-3 phosphorylation targets and the major paired helical filament (PHF) sites found in NFTs. Overexpression of FG01 significantly decreased tau phosphorylation at these GSK-3 target sites and increased unphosphorylated tau levels without affecting total tau levels (Figure 5E). These results suggest a role for FG01 in reducing tau phosphorylation, in addition to its effect on A β levels. We also analyzed protein levels and activity of CDK5, another kinase mediating tau phosphorylation in AD (Flaherty et al., 2000), following FG01 overexpression and observed little change, suggesting that CDK5 is not involved in FG01-regulated tau phosphorylation (Figure S5).

FG01 Interacts with Adenylate Cyclases to Upregulate cAMP Levels and PKA Activity

Inhibition of GSK-3 activity via phosphorylation of serine 21 in GSK-3 α and serine 9 in GSK-3 β can be mediated by protein kinase A (PKA) (Fang et al., 2000), so we studied whether FG01 regulates PKA activity. *In vitro* kinase assays revealed that FG01-transfected cells had significantly more PKA activity than control cells (Figure 6A), consistent with the observation that FG01 overexpression increased phosphorylation of CREB, a PKA substrate (Figure 6B). In addition, FG01 failed to inhibit GSK-3 activity and A β generation when PKA activity was suppressed by the specific inhibitor H89 (Figure 6B). Furthermore, downregulation of endogenous FG01 expression in N2aSwe cells by RNA interference (Figures 6C and 6D) dramatically reduced CREB phosphorylation, and increased GSK-3 activity and A β generation (Figure 6D). These data indicate that FG01's effects on GSK-3 activity and A β levels require PKA activation. Moreover, increased sAPP α secretion upon FG01 overexpression (Figure 5A) is also likely due to PKA activation, because PKA can stimulate budding of APP-containing vesicles from the Trans-Golgi Network (TGN) to cell surface, the major site for APP cleavage by α -secretase, therefore facilitating sAPP α generation (Xu et al., 1996).

Since cAMP binds to and activates PKA (Taylor et al., 2008), we investigated whether FG01 overexpression had any effect on cAMP levels. We found that FG01 overexpression significantly increased cAMP levels in both mouse N2a (38%) and rat PC12 (75%) cells (Figure 6E). We next examined potential interaction between FG01 and adenylate cyclases, enzymes responsible for cAMP synthesis (Kamenetsky et al., 2006). Co-immunoprecipitation studies showed that FG01 interacts with both overexpressed (data not shown) and endogenous (Figure 6F) adenylate cyclases in N2a cells overexpressing FG01, suggesting a possible modulation of enzymatic activity for cAMP production.

To confirm that it is indeed FG01 protein rather than *Fg01* mRNA that mediates these effects, we constructed an *Fg01* cDNA mutant vector with a stop codon at the beginning of the protein-coding region. Cells transfected with this mutant vector showed mRNA expression (detected by RT-PCR) but no protein expression of the mutant *Fg01* (Figure S6). In addition, overexpression of this mutant *Fg01* did not affect the activity of PKA or GSK-3, or A β levels (Figure S6), excluding any potential RNA interfering effects arising from anti-sense interaction with *Rps23* RNA.

Overexpression of FG01 Reduces A β Levels, GSK-3 Activity and Tau Phosphorylation in the Brain of the Triple Transgenic AD Mice

To validate FG01 function *in vivo*, we generated an *Fg01* transgenic mouse model specifically overexpressing Myc-tagged FG01 in the brain. A transgenic expression cassette driven by the human *Thy-1* promoter (Figure S7A) was microinjected into C57Bl6 mice and we used primers specifically amplifying exogenous *Fg01* to genotype transgenic mice (Figure S7B). Reverse transcription-PCR revealed that mRNA of the exogenous gene was indeed expressed in transgenic mouse brains (Figure S7C). Protein expression of exogenous Myc-tagged FG01 was also confirmed in brain tissues of transgenic mice (Figure S7D). In addition, immunoprecipitation/Western blot showed that total (including exogenous and endogenous) protein levels of FG01 in the transgenic mice were about two-fold higher than endogenous FG01 levels in control mice (Figure S7E). We generated two mouse lines with similar FG01 expression levels and results obtained from the two lines (including their crossing with 3XTg mice as described below) were similar. Herein we only presented results from line 2. Our results showed that levels of phosphorylated and therefore inactive GSK-3 α/β were increased (Figure S7D), accompanied by reduced GSK-3 β activity in *Fg01* transgenic mouse brain (Figure S7F). Increased CREB phosphorylation indicative of upregulated PKA activity, as well as decreased phosphorylation of endogenous mouse brain

tau, was also seen in *Fg01* transgenic mouse brain (Figure S7D). In addition, preliminary observation detected no obvious aberrant behavioral phenotypes in *Fg01* transgenic mice (data not shown).

We next crossed *Fg01* transgenic mice with triple transgenic (3XTg) AD mice harboring mutations in human *App* (APP), *Mapt* (tau) and *Psen1* (presenilin 1) genes (Oddo et al., 2003). As expected, FG01 overexpression in 3XTg mice dramatically increased the levels of cAMP and PKA activity (Figure S8A), resulting in elevated CREB activity, and reduced GSK-3 activity, tau phosphorylation, and A β levels in mouse brains (Figures 7A and S8B). Consistently, the numbers of both A β -immunostaining-positive (by A β 40-specific antibody and 6E10 antibody) and phosphorylated tau-immunostaining-positive (by PHF-1 and pT205 antibodies) neurons in the 3XTg mouse brain (both hippocampus and cortex) were significantly decreased following FG01 overexpression (Figures 7B, 7C, 7E, S8C, S8D, and S8F). Interestingly, protein levels of the synaptic marker PSD-95 were markedly increased following FG01 overexpression in 3XTg mouse brains (Figure 7A). Immunostaining of PSD-95 (Figures 7D and 7E) and synapsin (Figures S8E and S8F), another synaptic marker, also revealed significantly higher immunoreactivity in the hippocampus of 3XTg mouse brains with FG01 overexpression than that seen in 3XTg mice without FG01. These results imply that FG01 may rescue synapse impairment seen in 3XTg mice (Oddo et al., 2003), in addition to, or as a consequence of, its effects on reducing A β generation and tau phosphorylation. Consistent with the results found in cell cultures (Figure S4B), protein levels of ADAM10 and TACE were not affected by FG01 overexpression in the brain of 3XTg mice (Figure 7A).

Caloric restriction and environmental enrichment have been shown to reduce AD-like pathologies and behavior deficits in animal models (Halagappa et al., 2007; Lazarov et al., 2005). Since elevated CREB activity in the brain may affect animal behaviors such as food intake and daily activity, we compared body weight of FG01-overexpressing mice to that of control mice and found no difference at 3 months of age. At 7 and 11 months of age, we noticed that FG01-overexpressing mice are slightly (but not significantly) lighter than controls (data not shown), even though visual inspection of daily activity and food intake between these mice showed no obvious differences. Therefore, there is a possibility that FG01 exerts its effect on alleviating AD-like pathologies by altering mouse behaviors and this possibility deserves further investigation.

DISCUSSION

Using the RHGP assay to screen for genes involved in regulating A β generation, we identified the functional retroposed *Fg01* gene on mouse chromosome 8. The FG01 protein is a type Ib transmembrane protein and is expressed in the brain. In the present report, we provide compelling evidence to show that FG01 overexpression can reduce both A β levels and tau phosphorylation, two major pathological hallmarks of AD. We also reveal the underlying mechanism, i.e. FG01 interacts with adenylate cyclases to upregulate cAMP levels, which activates PKA activity, hence inhibiting GSK-3 activity, tau phosphorylation and A β generation. These results elucidate an important link between adenylate cyclases and AD, which had not been illustrated previously.

Sequence analyses demonstrated that *Fg01* originated through retroposition of mouse *Rps23*, which recruited regulatory units and additional protein encoding fragments at the retroposition site and became functional (Figure 3A). The reversal in transcriptional direction of *Fg01* relative to the parental *Rps23* gene explains why there is no protein sequence similarity between FG01 and RPS23. *Rps23* belongs to the ribosomal protein family and is highly conserved among species (Hori et al., 1993). Since human ribosomal

protein genes have been found to generate a large number of processed pseudogenes through retroposition (Zhang et al., 2002), there is a possibility that human *Rps23* may have also retroposed in humans and generated new functional genes with orientations and functions similar to that of *Fg01*. However, although we indeed identified several human *Rps23* retroposition sites in the human genome (Figure S1), neither computational gene prediction nor RT-PCR with primers binding adjacent regions of these human *Rps23* retroposition sites revealed any *Fg01-like* genes (data not shown), suggesting that the possibility that humans possess functional *Fg01* homologs is low.

During aging, humans are susceptible to AD pathogenesis, typically characterized by A β overproduction/aggregation and tau hyperphosphorylation. In contrast, wild type mice rarely develop AD pathologies (De Strooper et al., 1995; Jankowsky et al., 2007; Johnstone et al., 1991). The differences in AD susceptibility between humans and mice have been attributed to the sequence disparity between human and mouse A β (and possibly tau) that underlie different aggregation properties (De Strooper et al., 1995; Jankowsky et al., 2007; Johnstone et al., 1991), to the short lifespan of mice relative to humans (Jankowsky et al., 2004; Jankowsky et al., 2007), and to the differences in processing of human and mouse APP by BACE1 (Cai et al., 2001). Should humans lack *Fg01* homologs, our results would provide an alternative explanation, i.e. some genetic factors in mice, such as *Fg01*, protect them against an AD-like disease by preventing A β over-production and tau hyperphosphorylation.

On the other hand, mouse FG01 also exerts its functions in human cells, suggesting that FG01-mediated signaling pathways are active in humans. Further scrutiny of these pathways, especially upstream events involving FG01's effects on adenylate cyclases, is critical and underway. While it is not yet known whether there are functional analogs of FG01 in humans, further elucidation of FG01 functions and mechanism of action may prove to be important for developing new strategies for combating AD and other diseases including cancer and diabetes, in which the PKA and GSK-3 signaling pathways are centrally involved (Martinez et al., 2002; Naviglio et al., 2009).

EXPERIMENTAL PROCEDURES

Cells, Antibodies, and Reagents

Maintenance of mouse neuroblastoma N2a cells, N2a cells stably expressing human APP Swedish mutation (N2aSwe), human HeLa cells stably expressing human APP Swedish mutation (HeLaSwe), and rat PC12 cells has been described (Lin et al., 2007; Wang et al., 2006; York et al., 2000). Phoenix-Ampho helper cells were grown in Dulbecco's modified Eagle's medium supplemented with 10% fetal bovine serum. Antibodies used were: anti-Myc (9E10), anti-adenylate cyclases, anti-His, anti-ADAM10 and anti-TACE from Santa Cruz Biotechnology; anti-GSK-3 α , anti-GSK-3 β , anti-phospho-GSK-3 α/β (Ser21/9), anti-CREB, anti-phospho-CREB (Ser133), anti-PSD-95, and anti-synapsin from Cell Signaling Technology; anti-A β 40, anti-pT205 tau and anti-total tau from Abcam; anti-A β (6E10) from Covance; anti-tau-1 from Chemicon; anti- α -tubulin from Sigma; anti-PHF-1 tau from P. Davies at Albert Einstein School of Medicine; and the FCA18 antibody specifically recognizing the N-terminus of APP β CTF from F. Checler at Institut de Pharmacologie Moléculaire et Cellulaire du CNRS (Ancolio et al., 1999). The rabbit polyclonal antibody 369 against the APP C-terminus (Xu et al., 1997) and the anti-FG01 antibody were developed in our laboratory. PKA inhibitor H89 and GSK-3 inhibitor lithium chloride were from Sigma.

Random Homozygous Gene Perturbation (RHGP) Strategy for Screening A β -reducing Genes

We constructed a new RHGP gene search vector from the original pLLGSV vector (Li and Cohen, 1996). In both the 5'LTR and the 3'LTR regions of the new RHGP gene search vector, there is a sequence containing a puromycin N-acetyl-transferase gene (*pac*), a TRE (tetracycline-regulated element, *tet-off*) regulated CMV promoter driving the *pac* gene, a plasmid replication origin and a chloramphenicol resistance marker (Ori-CAT), and a *LoxP* site. In addition, there is a Cre recombinase gene (*Cre*) between the 5'LTR and the 3'LTR (Figure 1A). This new RHGP gene search vector was transfected into Phoenix-Ampho help cells. Generated infectious retrovirus in the cell culture supernatant was harvested and used to infect N2aSwe cells.

The infected N2aSwe cells with RHGP vector integration were selected with puromycin, live-stained with fluorescence-labeled APP β CTF antibody FCA18 (Ancolio et al., 1999), and subjected to multiple rounds of FACS sorting for cells with accumulated cell surface APP β CTF. The positive sorted cells were then treated with doxycycline (a derivative of tetracycline) and sorted for cells whose surface APP β CTF level was reversed back to background level in the presence of doxycycline. Resultant cells were cloned individually and assayed by ELISA and Western blotting to confirm surface accumulation of APP β CTF and reduction of A β generation. Positive candidate cell clones were further characterized and used for gene isolation.

Fg01 Gene Cloning

Genomic DNA was extracted from FG01 cells, digested with restriction enzyme *Bam*HI or *Hind*III, and self-ligated overnight with T4 ligase. The ligated DNA was precipitated, dissolved in TE buffer and electroporated into DH10B ElectroMax competent cells. The plasmid DNA from individual colonies was prepared for DNA sequencing. The target gene was identified by using UCSC Genome Browser Program.

Sequence Analysis

We blasted GenBank database with *Fg01* cDNA sequence to explore its origin. Homologous sequences between *Fg01* and mouse *Rps23* were aligned manually. Sequence similarity between *Fg01* and *Rps23* cDNA sequences of humans, mice and rats were compared using their homologous regions. Potential transmembrane region in the FG01 protein was predicted using PredictProtein (Rost et al., 2004).

Membrane Fractionation

N2a cells were transfected with FG01, APP or SMAD3 expression vectors (all Myc-tagged). After 48 hrs, cells were washed with ice-cold phosphate-buffered saline, collected with homogenization buffer (10 mM Tris-HCl, pH 7.4, 1 mM EDTA, 200 mM sucrose, 1 mM phenylmethylsulfonyl fluoride) and homogenized with a ball bearing cell cracker. Samples were centrifuged at $900 \times g$ for 10 min to remove cell debris and nuclei. Supernatants were centrifuged at $100,000 \times g$ for 60 min at 4°C. After transferring the supernatant (cytosol) to a new tube, the pellet was washed and re-suspended with an equal volume (to that of cytosol) of homogenization buffer.

Biotinylation

FG01 transfected N2a cells were washed with ice-cold phosphate-buffered saline containing 1 mM each of CaCl₂ and MgCl₂ and incubated at 4 °C with 0.5 mg/ml Sulfo-NHS-LC-biotin (Pierce) for 20 min and the process repeated once. Cell lysates were prepared in Nonidet P-40 lysis buffer. After affinity precipitation with streptavidin beads (Pierce),

biotinylated proteins were eluted with SDS-PAGE sample buffer (Invitrogen) and loaded directly on SDS-PAGE gels for electrophoresis followed by Western blot analysis with the Myc antibody.

Immunofluorescence Microscopy

For cell surface immunostaining of FG01, N2a cells were first transfected with the Myc-FG01-His₆ plasmid. Cells were then directly incubated with Myc or His₆ antibody at 4°C for 2 hrs, followed by washing, fixation, and permeabilization. In some experiments, cells were permeabilized before incubating with antibodies. Treated cells were incubated with Alexa Fluor 488-conjugated secondary antibody and DAPI. Specimens were examined and fluorescence images collected using a Zeiss fluorescence microscope with AxioVision software.

A β ELISA Assay

HeLaSwe cells were transfected with FG01 or controls. Conditioned media and lysates from these cells were collected. The levels of A β 40 and A β 42 were quantified using ELISA kits (Invitrogen), following the manufacturer's protocols.

Pharmacological Treatments

N2aSwe cells were transfected with control vector or FG01 and then equally split. Four hours before collection, cells were treated with the GSK-3 inhibitor lithium chloride (5 mM) or sodium chloride (5 mM, as control). Alternatively, cells were treated with a PKA inhibitor H89 (10 μ M) or with DMSO for control.

FG01 RNA Interference and Quantitative Real-Time PCR

The mouse FG01 siRNA used was: 5'-UACUGUUUGUCAUGCCACUUCUGAU-3'. The control siRNA was from Invitrogen. siRNA was transfected into N2a cells using Lipofectamine RNAiMAX reagent (Invitrogen), following the manufacturer's protocol. After FG01 RNA interference, total RNA was extracted from N2a cells by Trizol reagent (Invitrogen). After reverse transcription into first strand cDNA using standard conditions, samples were analyzed independently by real-time PCR using an iCycler iQ with SYBR green supermix (Bio-Rad). The FG01 primer pair used for real time PCR was: FG01-5' (5'-TGTTGCATACACATACATGC-3') and FG01-3' (5'-TCATTAAGAACGGGAAGAAG-3'). A pair of β -actin primers served as controls (Zhang et al., 2007).

In Situ Hybridization

Histological sections from 2-month-old C57Bl6 mice were used for *in situ* hybridization reactions. Digoxigenin-labeled sense and antisense probes were generated for *FG01* (corresponding to nucleotides 1–641 of NM_001024728), and the hybridization signal was detected using an alkaline-phosphatase-conjugated anti-digoxigenin antibody and BCIP/NTB (Roche).

Crossing Brain-Specific *Fg01* Transgenic Mice with 3XTg AD Mice

We generated brain-specific *Fg01* transgenic mice (Figure S7). Hemizygous *Fg01* transgenic mice were crossed with homozygous triple transgenic (3XTg) AD mice harboring mutations in human *App* and *Mapt* (tau) genes on a presenilin 1 (PS1) mutant background (Oddo et al., 2003). Procedures involving animals and their care conformed to institutional guidelines (Animal Resources Department at Burnham Institute for Medical Research).

Immunohistochemistry and Data Analyses

Fg01/3XTg mice and littermate controls on a 3XTg background were sacrificed at 11 months of age. Half of the brain was used for immunoblot analysis and the other half was paraffin-embedded for immunohistochemistry. Coronal brain sections (4 μ m) were deparaffinized, hydrated, and then immunostained with anti-A β antibodies (an anti-A β 40 specific antibody and 6E10), anti-phosphorylated tau antibodies (PHF-1 and pT205), or antibodies against PSD-95 and synapsin. After additional incubation with biotinylated secondary antibody, samples were incubated in ABC Elite (HRP) reagent (Vector Laboratories). Reactions were visualized by developing in DAB substrates (Vector Laboratories). All samples were visualized under a light microscope.

For immunohistochemistry comparison of A β and tau, immunostained neurons (>400) in were counted from five randomly selected cortical regions. Ratios of A β -positive and phosphorylated tau-positive neurons to total neurons were determined and normalized to those of controls. For immunohistochemistry comparison of synapse markers, five hippocampal regions were randomly selected and the images captured. After converting the images to grayscale, the optical density (darkness) of molecular layer staining was measured as an average of the gray value between white (0) and black (255) as described (Mathern et al., 1997) for comparison, by a computer-based image analysis using the Photoshop software.

In Vitro Activity Assays and cAMP Assay

Commercial kits were used to assay *in vitro* activities of GSK-3 β (Sigma) and PKA (Upstate). For GSK-3 α activity, a commercial GSK-3 β activity assay kit was used but the procedure to immunoprecipitate GSK-3 β was replaced with immunoprecipitation of GSK-3 α using an anti-GSK-3 α antibody (Cell Signaling). cAMP levels were assayed using a commercial kit (Biovision).

Co-immunoprecipitation

Cells transfected with FG01 were lysed in either CHAPSO buffer (1% CHAPSO, 25 mM HEPES, pH7.4, 150 mM NaCl, and 2mM EDTA supplemented with protease inhibitors) or in NP40 buffer (1% NP40 in phosphate buffered saline, supplemented with protease inhibitors). Lysates were immunoprecipitated using mouse IgG, rabbit IgG, and antibodies against Myc or adenylate cyclases and Trueblot™ IP beads (eBioscience), followed by Western blot with antibodies against Myc or adenylate cyclases.

Supplementary Material

Refer to Web version on PubMed Central for supplementary material.

Acknowledgments

We thank H. Zheng for providing the pHZ04 construct and helpful discussion, Y. M. Li for technical help, F. LaFerla for providing the 3XTg AD mice, F. Checler for providing the FCA18 antibody, and P. Davies for providing the PHF-1 tau antibody. This work was supported in part by National Institutes of Health grants (R01 AG021173 to H.X. and L.L.; R01 NS046673 and R01 AG030197 to H.X.; R01 NS054880 to F-F. L.; P01 AG009464 to P.G.), and grants from the Alzheimer's Association (to H.X. and F-F.L.), the American Health Assistance Foundation (to H.X.), US Department of Health and Human Services (AOA 90AZ2791 to P.G.), Fisher Center for Alzheimer's Research Foundation (to P.G.), Cure Alzheimer's Fund (to P.G.), National Natural Science Foundation of China (30672198 and 30840036 to Y.-w.Z.), National S&T Major Project (2009ZX09103-731 to Y.-w.Z.), and Natural Science Funds for Distinguished Young Scholar of Fujian Province (2009J06022 to Y.-w.Z.). Y.-w.Z. is supported by the Program for New Century Excellent Talents in Universities (NCET) and the Program for the New Century Excellent Talents in Fujian Province Universities (NCETFJ).

REFERENCES

- Ancolio K, Dumanchin C, Barelli H, Warter JM, Brice A, Campion D, Frebourg T, Checler F. Unusual phenotypic alteration of beta amyloid precursor protein (betaAPP) maturation by a new Val-715 --> Met betaAPP-770 mutation responsible for probable early-onset Alzheimer's disease. *Proc. Natl. Acad. Sci. USA.* 1999; 96:4119–4124. [PubMed: 10097173]
- Babushok DV, Ostertag EM, Kazazian HH Jr. Current topics in genome evolution: molecular mechanisms of new gene formation. *Cell. Mol. Life. Sci.* 2007; 64:542–554. [PubMed: 17192808]
- Barelli H, Lebeau A, Vizzavona J, Delaere P, Chevallier N, Drouot C, Marambaud P, Ancolio K, Buxbaum JD, Khorkova O, et al. Characterization of new polyclonal antibodies specific for 40 and 42 amino acid-long amyloid beta peptides: their use to examine the cell biology of presenilins and the immunohistochemistry of sporadic Alzheimer's disease and cerebral amyloid angiopathy cases. *Mol. Med.* 1997; 3:695–707. [PubMed: 9392006]
- Buee L, Bussiere T, Buee-Scherrer V, Delacourte A, Hof PR. Tau protein isoforms, phosphorylation and role in neurodegenerative disorders. *Brain Res. Brain Res. Rev.* 2000; 33:95–130. [PubMed: 10967355]
- Buxbaum JD, Ruefli AA, Parker CA, Cypess AM, Greengard P. Calcium regulates processing of the Alzheimer amyloid protein precursor in a protein kinase C-independent manner. *Proc. Natl. Acad. Sci. USA.* 1994; 91:4489–4493. [PubMed: 8183935]
- Cai H, Wang Y, McCarthy D, Wen H, Borchelt DR, Price DL, Wong PC. BACE1 is the major beta-secretase for generation of A β peptides by neurons. *Nat. Neurosci.* 2001; 4:233–234. [PubMed: 11224536]
- Chen F, Yang DS, Petanceska S, Yang A, Tandon A, Yu G, Rozmahel R, Ghiso J, Nishimura M, Zhang DM, et al. Carboxyl-terminal fragments of Alzheimer beta-amyloid precursor protein accumulate in restricted and unpredicted intracellular compartments in presenilin 1-deficient cells. *J. Biol. Chem.* 2000; 275:36794–36802. [PubMed: 10962005]
- Cole SL, Vassar R. The Alzheimer's disease beta-secretase enzyme BACE1. *Mol. Neurodegener.* 2007; 2:22. [PubMed: 18005427]
- De Strooper B, Aph-1, Pen-2, and Nicastrin with Presenilin generate an active gamma-Secretase complex. *Neuron.* 2003; 38:9–12. [PubMed: 12691659]
- De Strooper B, Simons M, Multhaup G, Van Leuven F, Beyreuther K, Dotti CG. Production of intracellular amyloid-containing fragments in hippocampal neurons expressing human amyloid precursor protein and protection against amyloidogenesis by subtle amino acid substitutions in the rodent sequence. *Embo J.* 1995; 14:4932–4938. [PubMed: 7588622]
- Fang X, Yu SX, Lu Y, Bast RC Jr, Woodgett JR, Mills GB. Phosphorylation and inactivation of glycogen synthase kinase 3 by protein kinase A. *Proc. Natl. Acad. Sci. USA.* 2000; 97:11960–11965. [PubMed: 11035810]
- Flaherty DB, Soria JP, Tomasiewicz HG, Wood JG. Phosphorylation of human tau protein by microtubule-associated kinases: GSK3 β and cdk5 are key participants. *J. Neurosci. Res.* 2000; 62:463–472. [PubMed: 11054815]
- Frame S, Cohen P. GSK3 takes centre stage more than 20 years after its discovery. *Biochem. J.* 2001; 359:1–16. [PubMed: 11563964]
- Gasparini L, Gouras GK, Wang R, Gross RS, Beal MF, Greengard P, Xu H. Stimulation of beta-amyloid precursor protein trafficking by insulin reduces intraneuronal beta-amyloid and requires mitogen-activated protein kinase signaling. *J. Neurosci.* 2001; 21:2561–2570. [PubMed: 11306609]
- Halagappa VK, Guo Z, Pearson M, Matsuoka Y, Cutler RG, Laferla FM, Mattson MP. Intermittent fasting and caloric restriction ameliorate age-related behavioral deficits in the triple-transgenic mouse model of Alzheimer's disease. *Neurobiol. Dis.* 2007; 26:212–220. [PubMed: 17306982]
- Hardy J, Selkoe DJ. The amyloid hypothesis of Alzheimer's disease: progress and problems on the road to therapeutics. *Science.* 2002; 297:353–356. [PubMed: 12130773]
- Hollis GF, Hieter PA, McBride OW, Swan D, Leder P. Processed genes: a dispersed human immunoglobulin gene bearing evidence of RNA-type processing. *Nature.* 1982; 296:321–325. [PubMed: 6801526]

- Hori N, Murakawa K, Matoba R, Fukushima A, Okubo K, Matsubara K. A cDNA sequence of human ribosomal protein, homologue of yeast S28. *Nucleic Acids Res.* 1993; 21:4394. [PubMed: 8415000]
- Jankowsky JL, Fadale DJ, Anderson J, Xu GM, Gonzales V, Jenkins NA, Copeland NG, Lee MK, Younkin LH, Wagner SL, et al. Mutant presenilins specifically elevate the levels of the 42 residue beta-amyloid peptide in vivo: evidence for augmentation of a 42-specific gamma secretase. *Hum. Mol. Genet.* 2004; 13:159–170. [PubMed: 14645205]
- Jankowsky JL, Younkin LH, Gonzales V, Fadale DJ, Slunt HH, Lester HA, Younkin SG, Borchelt DR. Rodent A beta modulates the solubility and distribution of amyloid deposits in transgenic mice. *J. Biol. Chem.* 2007; 282:22707–22720. [PubMed: 17556372]
- Jeffs P, Ashburner M. Processed pseudogenes in *Drosophila*. *Proc. Biol. Sci.* 1991; 244:151–159. [PubMed: 1679549]
- Johnstone EM, Chaney MO, Norris FH, Pascual R, Little SP. Conservation of the sequence of the Alzheimer's disease amyloid peptide in dog, polar bear and five other mammals by cross-species polymerase chain reaction analysis. *Brain Res. Mol. Brain Res.* 1991; 10:299–305. [PubMed: 1656157]
- Kaessmann H, Vinckenbosch N, Long M. RNA-based gene duplication: mechanistic and evolutionary insights. *Nat. Rev. Genet.* 2009; 10:19–31. [PubMed: 19030023]
- Kamenetsky M, Middelhaufe S, Bank EM, Levin LR, Buck J, Steegborn C. Molecular details of cAMP generation in mammalian cells: a tale of two systems. *J. Mol. Biol.* 2006; 362:623–639. [PubMed: 16934836]
- Karin M, Richards RI. Human metallothionein genes--primary structure of the metallothionein-II gene and a related processed gene. *Nature.* 1982; 299:797–802. [PubMed: 7133118]
- Kopan R, Goate A. A common enzyme connects notch signaling and Alzheimer's disease. *Genes Dev.* 2000; 14:2799–2806. [PubMed: 11090127]
- Lazarov O, Robinson J, Tang YP, Hairston IS, Korade-Mirnic Z, Lee VM, Hersh LB, Sapolsky RM, Mirnic K, Sisodia SS. Environmental enrichment reduces Abeta levels and amyloid deposition in transgenic mice. *Cell.* 2005; 120:701–713. [PubMed: 15766532]
- Lee VM, Goedert M, Trojanowski JQ. Neurodegenerative tauopathies. *Annu. Rev. Neurosci.* 2001; 24:1121–1159. [PubMed: 11520930]
- Li L, Cohen SN. Tsg101: a novel tumor susceptibility gene isolated by controlled homozygous functional knockout of allelic loci in mammalian cells. *Cell.* 1996; 85:319–329. [PubMed: 8616888]
- Lih CJ, Wei W, Cohen SN. Tsr1: a transcriptional regulator of thrombospondin-1 that modulates cellular sensitivity to taxanes. *Genes Dev.* 2006; 20:2082–2095. [PubMed: 16847352]
- Lin P, Li F, Zhang YW, Huang H, Tong G, Farquhar MG, Xu H. Calnuc binds to Alzheimer's beta-amyloid precursor protein and affects its biogenesis. *J. Neurochem.* 2007; 100:1505–1514. [PubMed: 17348862]
- Liu K, Li L, Cohen SN. Antisense RNA-mediated deficiency of the calpain protease, nCL-4, in NIH3T3 cells is associated with neoplastic transformation and tumorigenesis. *J. Biol. Chem.* 2000a; 275:31093–31098. [PubMed: 10906334]
- Liu K, Li L, Nisson PE, Gruber C, Jessee J, Cohen SN. Reversible tumorigenesis induced by deficiency of vasodilator-stimulated phosphoprotein. *Mol. Cell. Biol.* 1999; 19:3696–3703. [PubMed: 10207093]
- Liu K, Li L, Nisson PE, Gruber C, Jessee J, Cohen SN. Neoplastic transformation and tumorigenesis associated with sam68 protein deficiency in cultured murine fibroblasts. *J. Biol. Chem.* 2000b; 275:40195–40201. [PubMed: 11032831]
- Long M, Betran E, Thornton K, Wang W. The origin of new genes: glimpses from the young and old. *Nat. Rev. Genet.* 2003; 4:865–875. [PubMed: 14634634]
- Martinez A, Castro A, Dorronsoro I, Alonso M. Glycogen synthase kinase 3 (GSK-3) inhibitors as new promising drugs for diabetes, neurodegeneration, cancer, and inflammation. *Med. Res. Rev.* 2002; 22:373–384. [PubMed: 12111750]
- Mathern GW, Bertram EH 3rd, Babb TL, Pretorius JK, Kuhlman PA, Spradlin S, Mendoza D. In contrast to kindled seizures, the frequency of spontaneous epilepsy in the limbic status model

correlates with greater aberrant fascia dentata excitatory and inhibitory axon sprouting, and increased staining for N-methyl-D-aspartate, AMPA and GABA(A) receptors. *Neuroscience*. 1997; 77:1003–1019. [PubMed: 9130782]

- Medina M, Castro A. Glycogen synthase kinase-3 (GSK-3) inhibitors reach the clinic. *Curr. Opin. Drug Discov. Devel.* 2008; 11:533–543.
- Mighell AJ, Smith NR, Robinson PA, Markham AF. Vertebrate pseudogenes. *FEBS Lett.* 2000; 468:109–114. [PubMed: 10692568]
- Naviglio S, Caraglia M, Abbruzzese A, Chiosi E, Di Gesto D, Marra M, Romano M, Sorrentino A, Sorvillo L, Spina A, Illiano G. Protein kinase A as a biological target in cancer therapy. *Expert Opin. Ther. Targets.* 2009; 13:83–92. [PubMed: 19063708]
- Oddo S, Caccamo A, Shepherd JD, Murphy MP, Golde TE, Kaye R, Metherate R, Mattson MP, Akbari Y, LaFerla FM. Triple-transgenic model of Alzheimer's disease with plaques and tangles: intracellular Abeta and synaptic dysfunction. *Neuron.* 2003; 39:409–421. [PubMed: 12895417]
- Phiel CJ, Wilson CA, Lee VM, Klein PS. GSK-3alpha regulates production of Alzheimer's disease amyloid-beta peptides. *Nature.* 2003; 423:435–439. [PubMed: 12761548]
- Rost B, Yachdav G, Liu J. The PredictProtein server. *Nucleic Acids Res.* 2004; 32:W321–W326. [PubMed: 15215403]
- Takashima A, Yamaguchi H, Noguchi K, Michel G, Ishiguro K, Sato K, Hoshino T, Hoshi M, Imahori K. Amyloid beta peptide induces cytoplasmic accumulation of amyloid protein precursor via tau protein kinase I/glycogen synthase kinase-3 beta in rat hippocampal neurons. *Neurosci. Lett.* 1995; 198:83–86. [PubMed: 8592647]
- Tanzi RE, Bertram L. Twenty years of the Alzheimer's disease amyloid hypothesis: a genetic perspective. *Cell.* 2005; 120:545–555. [PubMed: 15734686]
- Taylor SS, Kim C, Cheng CY, Brown SH, Wu J, Kannan N. Signaling through cAMP and cAMP-dependent protein kinase: diverse strategies for drug design. *Biochim. Biophys. Acta.* 2008; 1784:16–26. [PubMed: 17996741]
- Ueda S, Nakai S, Nishida Y, Hisajima H, Honjo T. Long terminal repeat-like elements flank a human immunoglobulin epsilon pseudogene that lacks introns. *Embo J.* 1982; 1:1539–1544. [PubMed: 6327276]
- Vinckenbosch N, Dupanloup I, Kaessmann H. Evolutionary fate of retroposed gene copies in the human genome. *Proc. Natl. Acad. Sci. USA.* 2006; 103:3220–3225. [PubMed: 16492757]
- Wang R, Zhang YW, Zhang X, Liu R, Zhang X, Hong S, Xia K, Xia J, Zhang Z, Xu H. Transcriptional regulation of APH-1A and increased gamma-secretase cleavage of APP and Notch by HIF-1 and hypoxia. *Faseb J.* 2006; 20:1275–1277. [PubMed: 16645044]
- Xu H, Gouras GK, Greenfield JP, Vincent B, Naslund J, Mazzarelli L, Fried G, Jovanovic JN, Seeger M, Relkin NR, et al. Estrogen reduces neuronal generation of Alzheimer beta-amyloid peptides. *Nat. Med.* 1998; 4:447–451. [PubMed: 9546791]
- Xu H, Sweeney D, Greengard P, Gandy S. Metabolism of Alzheimer beta-amyloid precursor protein: regulation by protein kinase A in intact cells and in a cell-free system. *Proc. Natl. Acad. Sci. USA.* 1996; 93:4081–4084. [PubMed: 8633020]
- Xu H, Sweeney D, Wang R, Thinakaran G, Lo AC, Sisodia SS, Greengard P, Gandy S. Generation of Alzheimer beta-amyloid protein in the trans-Golgi network in the apparent absence of vesicle formation. *Proc. Natl. Acad. Sci. USA.* 1997; 94:3748–3752. [PubMed: 9108049]
- York RD, Molliver DC, Grewal SS, Stenberg PE, McCleskey EW, Stork PJ. Role of phosphoinositide 3-kinase and endocytosis in nerve growth factor-induced extracellular signal-regulated kinase activation via Ras and Rap1. *Mol. Cell. Biol.* 2000; 20:8069–8083. [PubMed: 11027277]
- Zhang X, Zhou K, Wang R, Cui J, Lipton SA, Liao FF, Xu H, Zhang YW. Hypoxia-inducible factor 1alpha (HIF-1alpha)-mediated hypoxia increases BACE1 expression and beta-amyloid generation. *J. Biol. Chem.* 2007; 282:10873–10880. [PubMed: 17303576]
- Zhang YW, Xu H. Molecular and Cellular Mechanisms for Alzheimer's Disease: Understanding APP Metabolism. *Curr. Mol. Med.* 2007; 7:687–696. [PubMed: 18045146]
- Zhang Z, Carriero N, Gerstein M. Comparative analysis of processed pseudogenes in the mouse and human genomes. *Trends Genet.* 2004; 20:62–67. [PubMed: 14746985]

Zhang Z, Harrison P, Gerstein M. Identification and analysis of over 2000 ribosomal protein pseudogenes in the human genome. *Genome Res.* 2002; 12:1466–1482. [PubMed: 12368239]

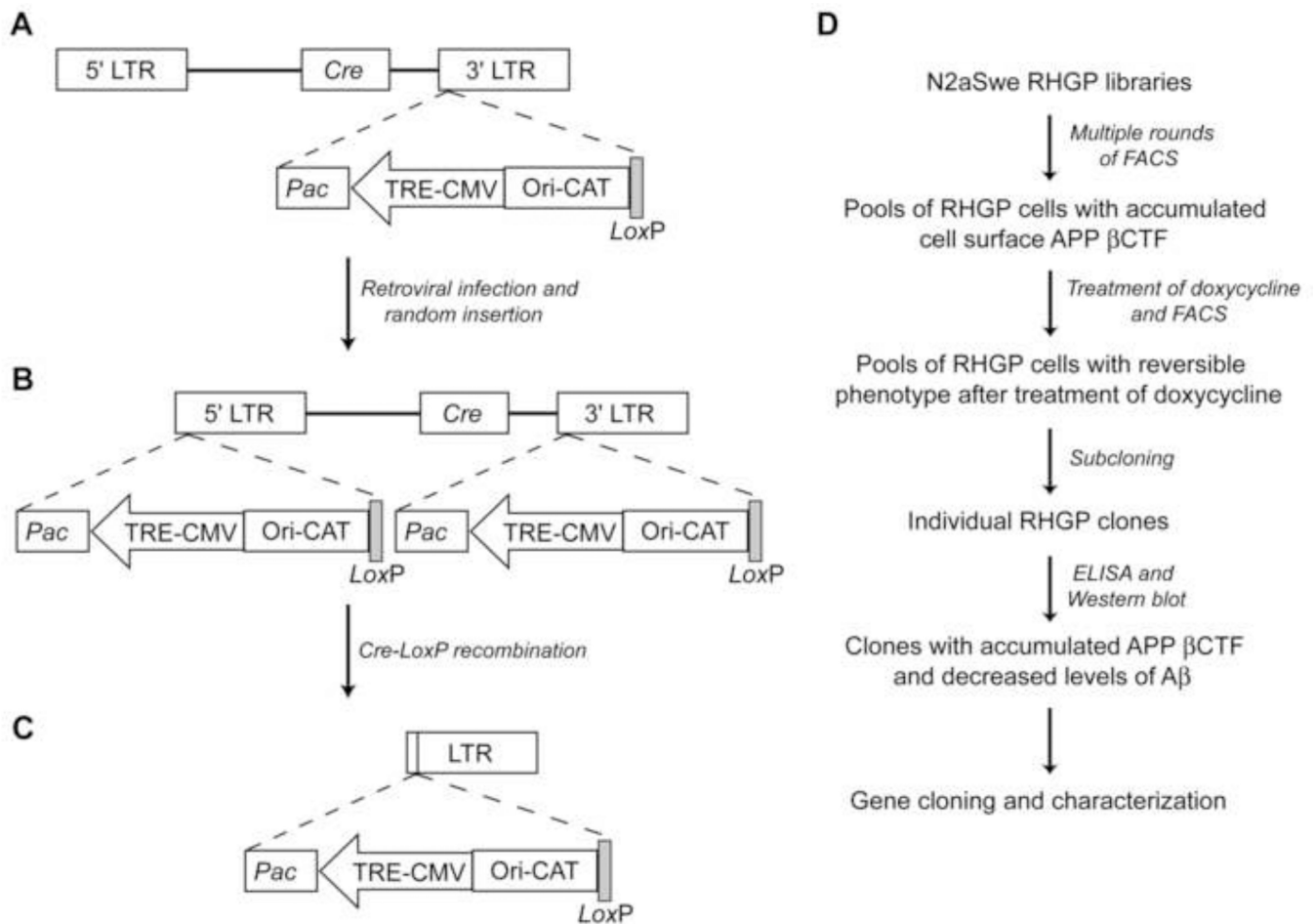


Figure 1. Genetic Screening Using Random Homozygous Gene Perturbation (RHGP)

(A) The new RHGP gene search vector has a tetracycline-regulated element (TRE) regulated CMV promoter, which drives expression of the puromycin N-acetyl-transferase gene (*pac*), a plasmid replication origin and a chloramphenicol resistance marker (Ori-CAT), and a *LoxP* site in both the 5'LTR (not shown) and the 3'LTR. In addition, there is a Cre recombinase gene (*Cre*) between the 5'LTR and the 3'LTR.

(B) The initial provirus randomly inserted into chromosomes of mammalian cells upon retroviral infection.

(C) The final integrated provirus after the expression of the *Cre* recombinase in the initial provirus, which mediates DNA recombination at the *loxP* sites.

(D) Strategy for screening for Aβ-reducing genes in N2aSwe cells with RHGP vector integration.

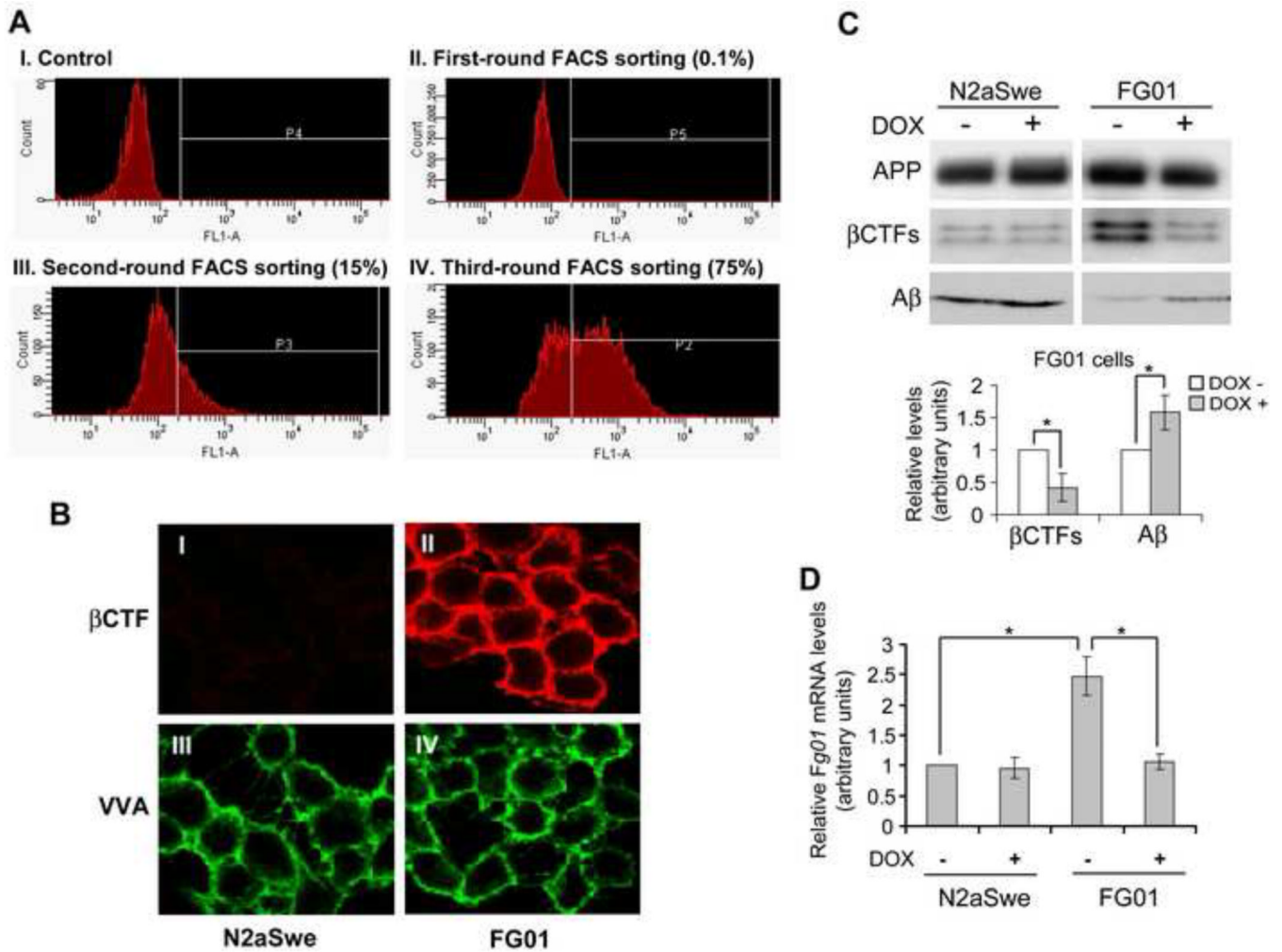


Figure 2. Identification of the FG01 Cell Clone

(A) RHGP libraries of N2aSwe cells were live-immunostained for cell surface β CTF using an A β N-terminal specific antibody (FCA18) (Barelli et al., 1997) and screened by multiple rounds of FACS sorting. Less than 0.01% of cells showing β CTF accumulation after first round of FACS sorting were enriched up to 75% following another two rounds of FACS sorting. Y axis, cell number; X axis, fluorescence intensity.

(B) Parental N2aSwe cells (I and III) and one cell clone derived from FACS sorting, FG01 (II and IV), were live-immunostained to visualize surface APP β CTF (red, I and II). Cells were also double immunostained with FITC-VVA (Vicia Vilosa Agglutinin, Vector Laboratories) to stain total surface glycoproteins (III and IV).

(C) Parental N2aSwe and FG01 cells were treated with or without 2 μ g/ml doxycycline (DOX) for 72 hrs. Equal amounts of cell lysates were subjected to SDS-PAGE and Western blot to detect full length APP and β CTFs. Secreted A β was immunoprecipitated from conditioned media and analyzed by Western blot. Protein levels in FG01 cells were quantified by densitometry and normalized to those of controls for comparison (set as one arbitrary unit).

(D) Parental N2aSwe and FG01 cells were treated with 2 μ g/ml doxycycline (+) or DMSO (-) for 72 hrs before RNA was isolated for real-time reverse transcription-PCR to quantify *Fg01* expression. The level of *Fg01* in N2aSwe cells treated with DMSO was used as normalization controls (set as one arbitrary unit).

* $P < 0.05$. P values were calculated using two-tailed Student's t -test ($n = 3$). Error bars, SEM.

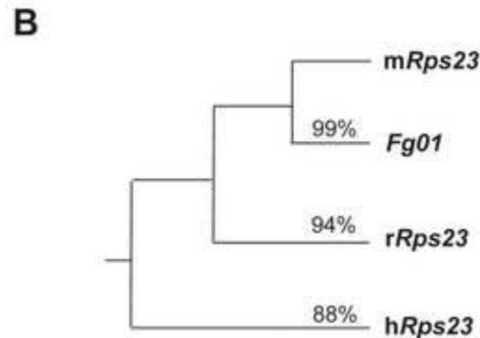
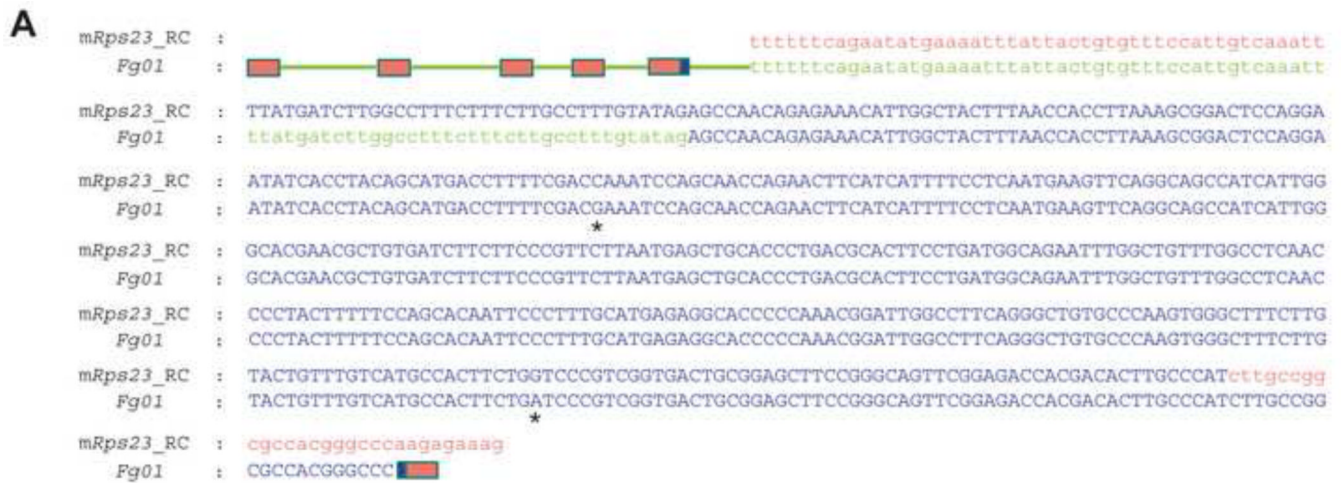


Figure 3. The *Fg01* Gene Originated Through Retroposition of the Mouse *Rps23* mRNA
 (A) Sequence alignment of the reverse and complementary (RC) sequence of mouse *Rps23* (*mRps23*) mRNA with *Fg01*. Small letters indicate intron sequence (in green) or untranslated regions of the exon (in red). Capital letters indicate protein-encoding sequence (in blue). Additional gene parts of *Fg01* recruited from integrated chromosomal sites were indicated by lines (for introns) and boxes (for exons) (not drawn to proportion). The colors red, green and blue indicate exons, introns, and protein-encoding regions, respectively. *: nonconserved nucleotide residues.
 (B) Phylogenetic relationships among *Fg01* and human, rat and mouse *Rps23* genes (*hRps23*, *rRps23*, and *mRps23*) based on their sequence identity to *mRps23* within the homologous region.

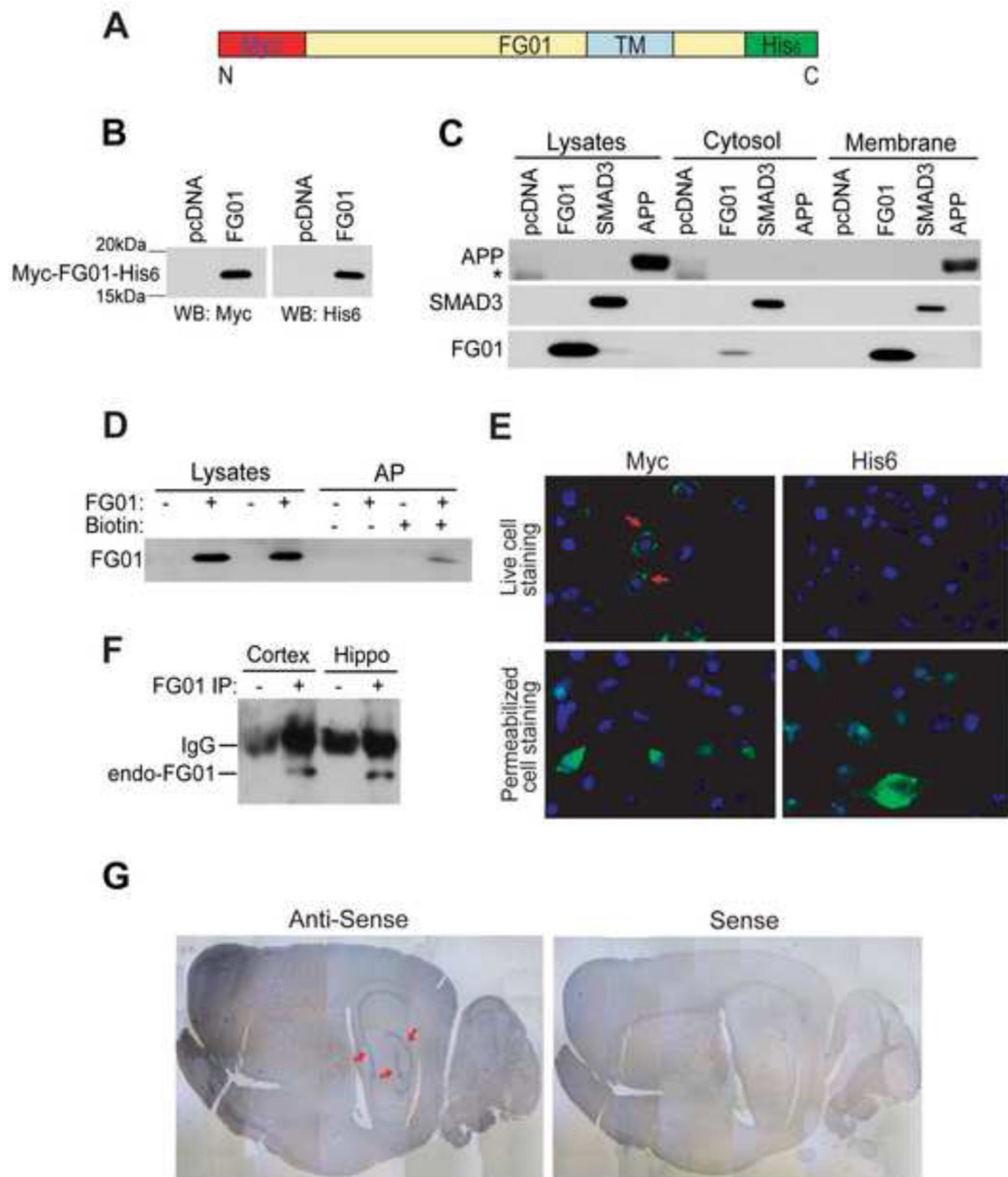


Figure 4. FG01 is a Type Ib Transmembrane Protein

(A) Scheme of the FG01 construct used in this study (not drawn to proportion), with a Myc tag at the N-terminus and a His₆ tag at the C-terminus. FG01 has a predicted single transmembrane domain (TM) near its C-terminus.

(B) The Myc-FG01-His₆ vector or a pcDNA control was transiently transfected into N2a cells. Cell lysates were subjected to Western blot (WB) with antibodies against Myc or His₆.

(C) FG01, APP and SMAD3 plasmids (all Myc-tagged) were individually transfected into N2a cells. After fractionation of membrane and cytosol, equal volumes of samples from both fractions were subjected to SDS-PAGE and Western analysis with a Myc antibody. *: non-specific band.

(D) After FG01 transfection, N2a cells were biotinylated and biotin-labeled membrane proteins were affinity precipitated (AP) with streptivadin and immunoblotted with a Myc antibody.

(E) After transfection with the Myc-FG01-His₆ construct, N2a cells were either live-immunostained or permeabilized and immunostained with Myc or His₆ antibody. Cells were then fixed, permeabilized, incubated with Alexa Fluor 488-conjugated secondary antibody and DAPI, and examined by immunofluorescence microscopy. Red arrows indicate membrane staining of FG01 in live cells.

(F) Equal protein lysates from mouse cortex and hippocampus (hippo) were incubated with an FG01 antibody (+) or rabbit IgG (-). After immunoprecipitation, samples were subjected to SDS-PAGE and Western blot analysis with the FG01 antibody.

(G) An anti-sense probe of *Fg01* and the corresponding sense probe (as control) were used for *in situ* hybridization in brain sections from a two-month-old C57Bl6 mouse. Red arrows indicate *Fg01* expression.

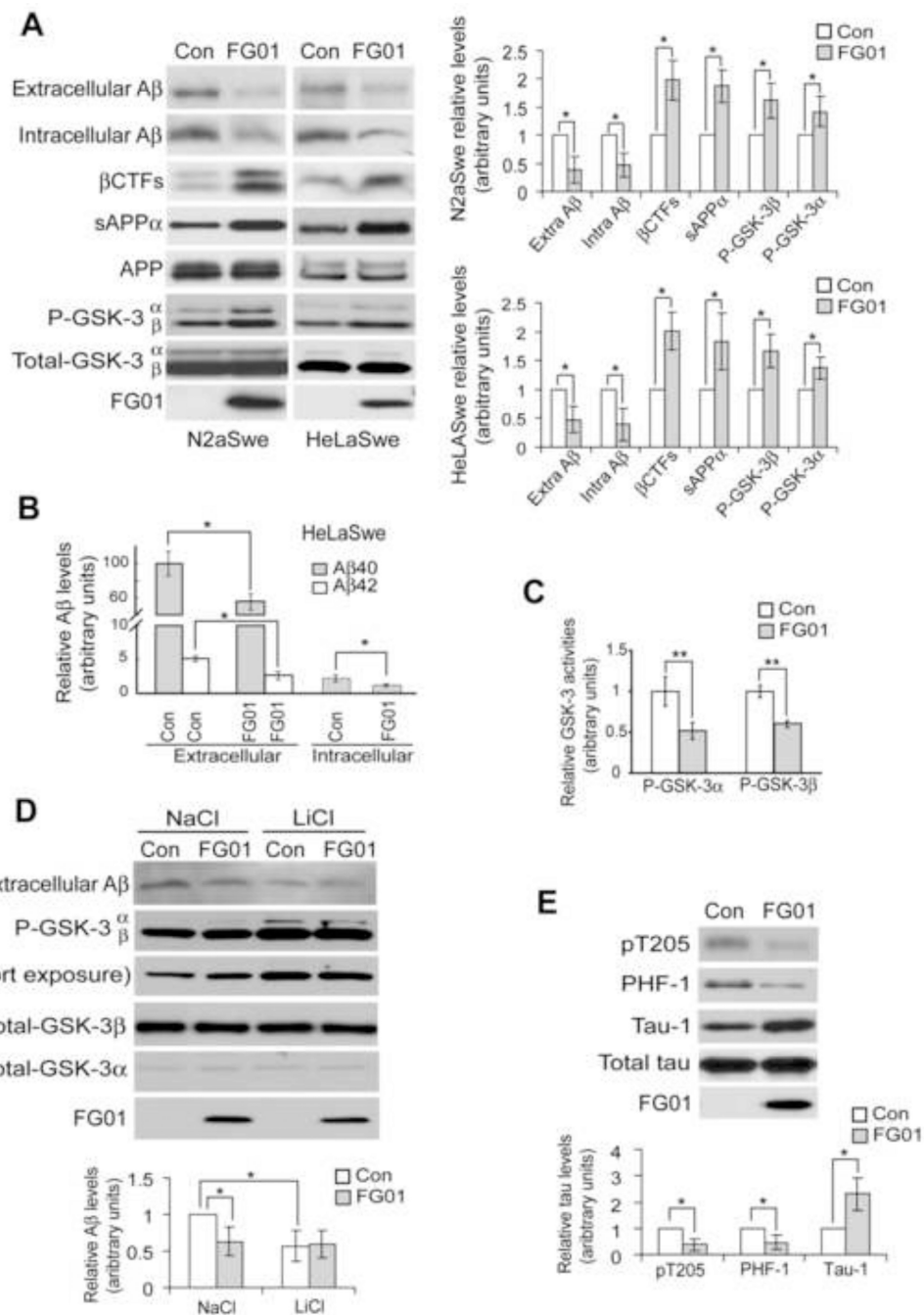


Figure 5. FG01 Reduces A β Levels, GSK-3 Activity and tau Phosphorylation

(A) FG01 or control vector (Con) were transfected into mouse N2aSwe or human HeLaSwe cells. A β in conditioned media (secreted or extracellular) and cell lysates (intracellular) was immunoprecipitated and Western blotted with the A β antibody 6E10. sAPP α in conditioned media was immunoblotted with 6E10. Cell lysates were immunoblotted with antibodies against APP/ β CTF (6E10), phosphorylated GSK-3 α/β , total GSK3 α/β , and Myc-FG01 (9E10).

(B) ELISA quantification of A β 40 and A β 42 levels in conditioned media and lysates of HeLaSwe cells with FG01 overexpression. Results were normalized to that of A β 40 in

conditioned media (set as 100). A β 42 in cell lysates was below detection level and not shown.

(C) GSK-3 α and GSK-3 β in lysates from N2aSwe cells transfected with control or FG01 cDNA were immunoprecipitated with respective antibodies and assayed for *in vitro* activity. Results were normalized to those of controls (set as one arbitrary unit).

(D) N2aSwe cells were first transfected with FG01 or control vector (Con). After equal splitting, cells were treated with 5 mM LiCl or NaCl (as control) for 4 hrs before collection. Conditioned media were assayed for A β . Cell lysates were analyzed for total and phosphorylated GSK-3 α/β and for FG01.

(E) N2a cells were transfected with human tau, equally split, and transfected with FG01 or control vector (Con). The levels of phosphorylated tau including threonine 205 (pT205) and PHF-1, unphosphorylated tau (Tau-1), total tau, and FG01 were analyzed.

In some experiments, protein levels were quantified by densitometry and normalized to those of controls for comparison (set as one arbitrary unit). All error bars indicate SEM.

* $P < 0.05$, ** $P < 0.01$. P values were calculated using two-tailed Student's t -test ($n = 3$).

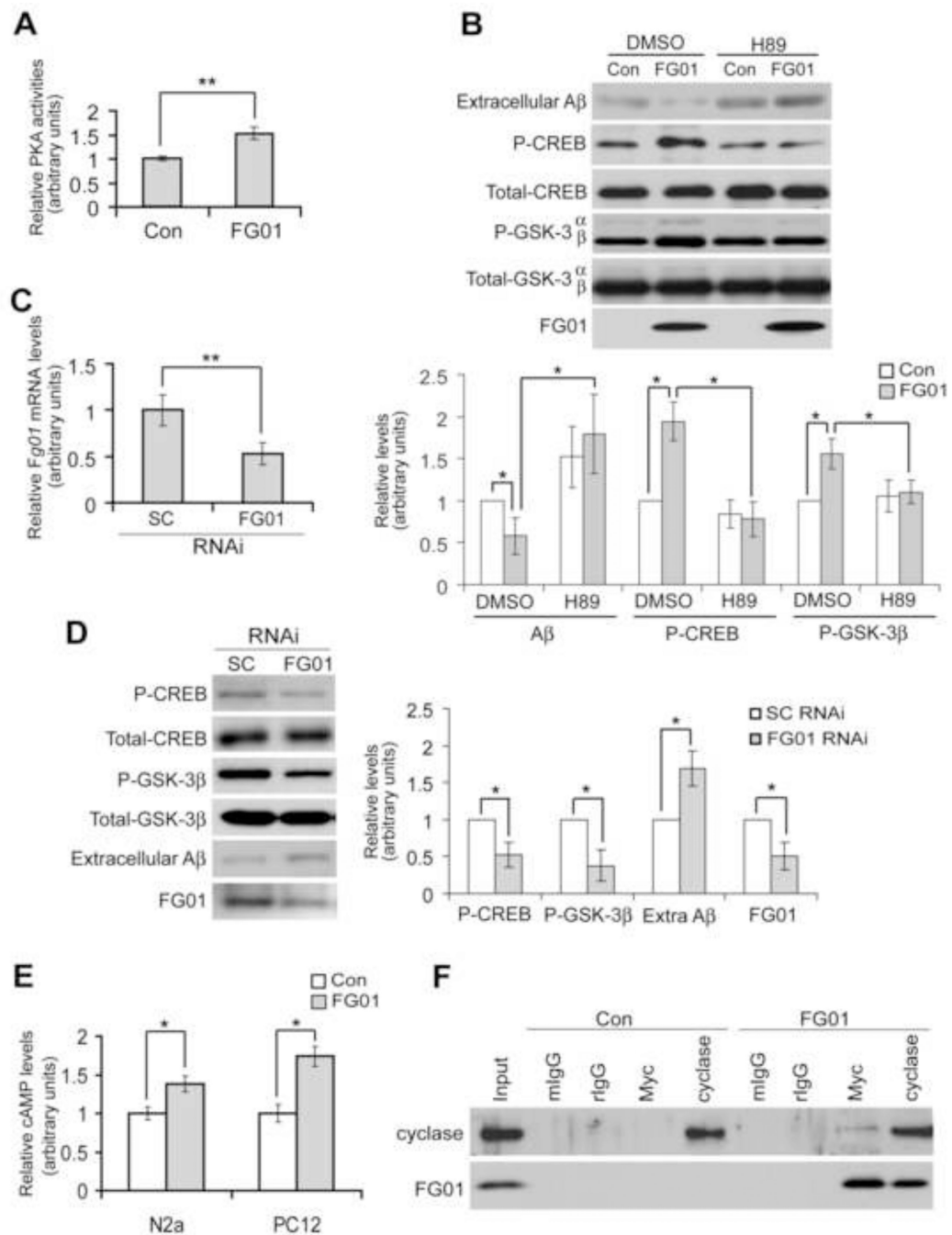


Figure 6. FG01 Interacts with Adenylate Cyclases, Upregulates cAMP Levels and Activates PKA to Reduce GSK-3 Activity and A β Levels

(A) Cells transfected with FG01 or control vector (Con) were analyzed for *in vitro* PKA activity. Results were normalized to control values (set as one arbitrary unit).

(B) After transfection with FG01 or control vectors (Con) and equal splitting, cells were treated with DMSO (control) or the PKA inhibitor H89. Conditioned media were analyzed for A β and cell lysates were analyzed for phosphorylated and total CREB, phosphorylated and total GSK-3, and FG01 levels.

(C) N2aSwe cells were transfected with *Fg01*-specific RNAi or a scrambled RNAi (SC). Total RNA was then extracted and subjected to RT-PCR. The level of *Fg01* relative to that

of β -actin was analyzed and normalized to that from scrambled RNAi-transfected cells (set as one arbitrary unit).

(D) After RNAi of *Fg01* expression, conditioned media from N2aSwe cells were analyzed for A β , and cell lysates were analyzed for endogenous FG01 and phosphorylated/total CREB and GSK-3.

(E) Mouse N2a and rat PC12 cells were transfected with FG01 or control vectors, and cell lysates were assayed for cAMP levels. Data were normalized to control values (as one arbitrary unit).

(F) Cells transfected with FG01 or control vectors were lysed in 1% CHAPSO or 1% NP40 buffer. Lysates were incubated with mouse IgG (mIgG), rabbit IgG (rIgG), Myc antibody or adenylate cyclase antibody. Immunoprecipitated proteins were subjected to SDS-PAGE and Western blot analysis with adenylate cyclase or Myc (for FG01) antibodies.

In some experiments, protein levels were quantified by densitometry and normalized to those of controls for comparison (set as one arbitrary unit). All error bars indicate SEM.

* $P < 0.05$, ** $P < 0.01$. P values were calculated using two-tailed Student's t -test ($n = 3$).

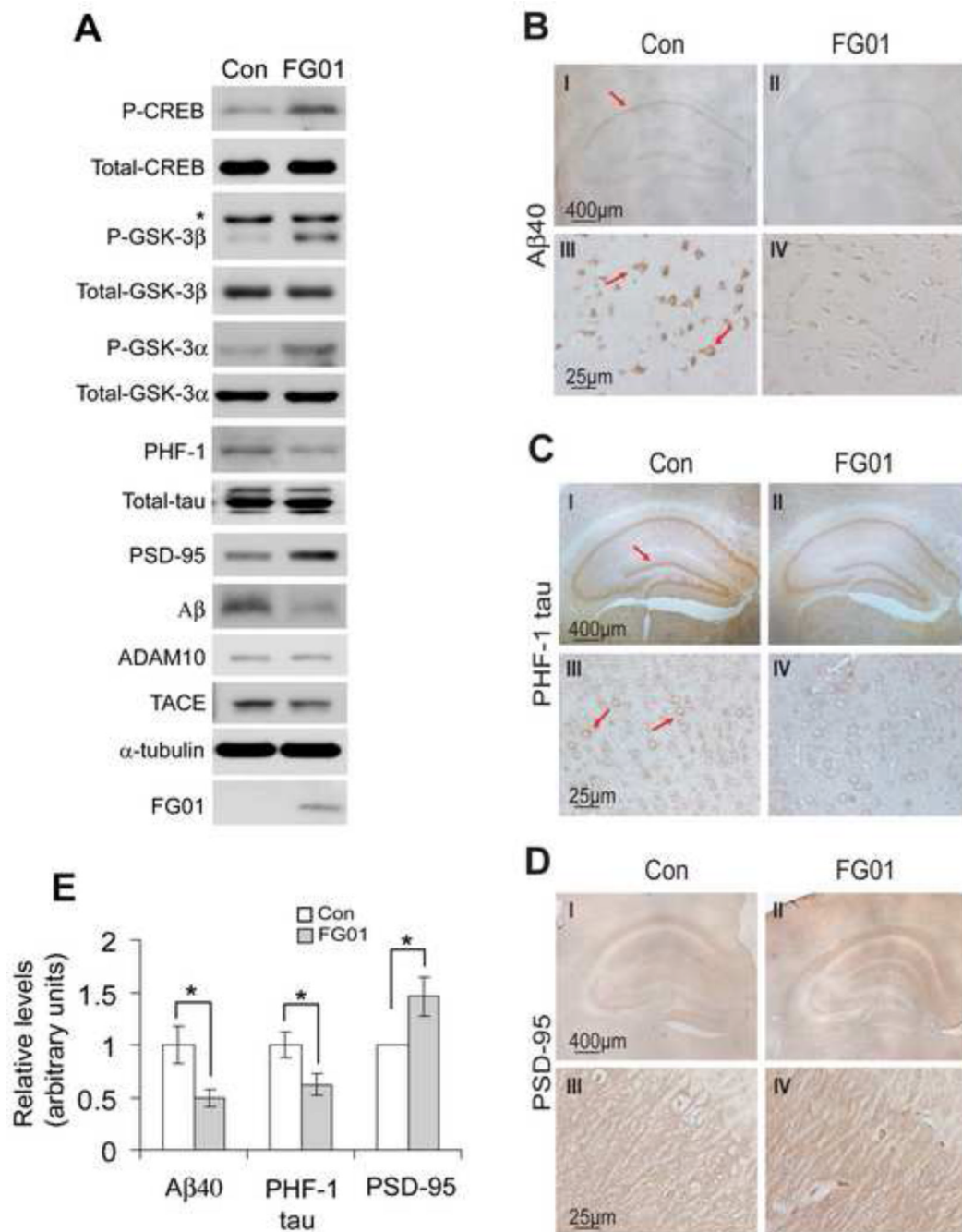


Figure 7. FG01 Overexpression Increases PKA Activity and Synapse number and Reduces GSK-3 β Activity, tau Phosphorylation, and A β Levels in Brains of 3XTg AD Mice

(A) Brains from FG01 mice and littermate controls (Con) on a 3XTg background at 11 months of age were dissected. One half of the brain was lysed and analyzed for the levels of phosphorylated/total CREB, phosphorylated/total GSK-3, PSD-95, ADAM10, TACE, α -tubulin, and phosphorylated (PHF-1) and total tau forms by direct Western blot. A β and Myc-FG01 were detected by immunoprecipitation-Western blot using A β antibody (6E10) and Myc antibody, respectively. *: non-specific band found specifically in 3XTg mouse brains.

(B) The other half brain from Con (I and III) and FG01 (II and IV) mice was analyzed by immunohistochemistry for A β using an A β 40-specific antibody. III and IV are higher magnifications of cortical regions from I and II, respectively. Red arrows indicate positive immunoreactivity.

(C) Immunohistochemistry for phosphorylated tau (PHF-1 tau) was analyzed the same as in (B). Red arrows indicate positive immunoreactivity.

(D) Immunohistochemistry for PSD-95 was analyzed the same as in (B), except that III and IV are higher magnifications of hippocampal regions from I and II, respectively.

(E) Immunostained neurons (>400) in (B) and (C) were counted from 5 randomly selected cortical regions. Ratios of A β 40-positive and PHF-1 tau-positive neurons to total neurons were determined and normalized to those of control (Con) for comparison. The optical density (darkness) of PSD-95 staining in 5 randomly selected hippocampal regions were analyzed by the Photoshop software for comparison. * P <0.05. P values were calculated using two-tailed Student's t -test ($n = 4$). Error bars, SEM.